The Polar Shell Renderer:

Equal-Area Denominator Shells for Reduced Fractions

and Primitive Roots of Unity

Jeffery Huckstead (Cerebral Graphix)
ORCID 0009-0007-0234-2177

Representation note — "a lens, not a law."
Revised July 9, 2026
DOI: 10.5281/zenodo.21280464

Abstract

We describe a polar rendering of the reduced fractions. Each reduced fraction k/n with $\gcd(k,n)=1$ is placed at radius $\sqrt{n}$ and angle $2\pi k/n$. Under this map *four* classical structures become visible together in a single figure: each concentric shell at radius $\sqrt{n}$ carries exactly $\varphi(n)$ points (Euler's totient); the angular positions on that shell are exactly the primitive n-th roots of unity (the roots of the n-th cyclotomic polynomial); the $\sqrt{n}$ radial law makes every denominator shell an equal-area annulus; and the cumulative point count out to denominator N is the summatory totient $\Phi(N)$, whose leading asymptotic $3N^2/\pi^2$ is the classical Mertens result (with Walfisz's later refinement of the error term) and whose value $1+\Phi(N)$ is the length of the Farey sequence of order N. Because shell n carries $\varphi(n)$ points rather than one, the rendering is *not* a constant-density filling of the disk; the equal-area claim is instead denominator-local, so each assigned annulus has area π and its annularly normalized population is $\varphi(n)/\pi$. All four facts are classical; the contribution is the specific unified representation and the equal-area-by-denominator choice that ties the number-theoretic content to the phyllotaxis (sunflower) tradition. We position the rendering among existing fraction- and root-visualizations — Ford circles, Farey-sunburst constructions, Vogel's sunflower, roots-of-unity diagrams, and the Ulam–Sacks prime spirals — and within the author's Triangular-Fractional Grid series, giving the exact denominator-collapse map that realizes the rendering as the reduced skeleton of that grid. No prior instance of the specific unified rendering was found, but the absence of a found instance is not a proof of novelty, and no arithmetical claim is made beyond the classical facts recalled.

Notation. Throughout, $\Phi_n(x)$ denotes the n-th cyclotomic polynomial, while $\Phi(N)=\sum_{n\le N}\varphi(n)$ denotes the summatory totient. The two are standard and distinct; they sit close together here, so the reader is asked to keep the subscript (Φ_n, a polynomial) apart from the argument ($\Phi(N)$, a counting function).

1 The construction

Fix the reduced fractions: the rationals k/n with $n\ge 1$, $1\le k\le n$, and $\gcd(k,n)=1$. (For $n=1$ the single fraction is $1/1$; for $n\ge 2$ the admissible numerators are the residues in $\{1,\dots,n-1\}$ coprime to n.) The polar shell renderer places each such fraction at the point with polar coordinates

$$r=\sqrt{n},\qquad \theta=\frac{2\pi k}{n},\qquad \text{equivalently}\qquad x=\sqrt{n}\cos\frac{2\pi k}{n},\ \ y=\sqrt{n}\sin\frac{2\pi k}{n}. \tag{1}$$

The denominator sets the radius; the numerator sets the angle. Points sharing a denominator n lie on a common circle of radius $\sqrt{n}$, which we call the *shell* of index n (Figure 1). We fix the orientation once and

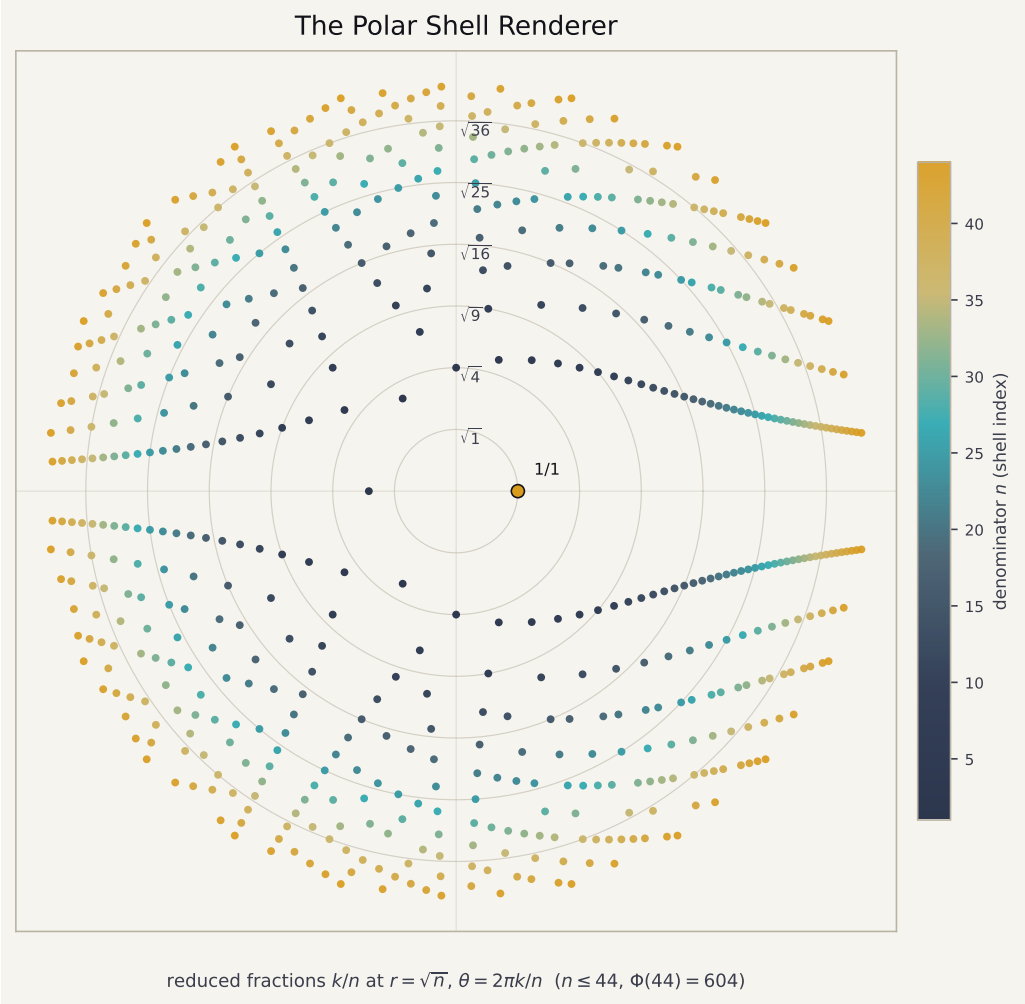

Figure 1: The polar shell renderer for denominators $n \leq 44$ (604 points $= \Phi(44)$). Each point is a reduced fraction k/n at $(\sqrt{n}, 2\pi k/n)$, colored by denominator n; $1/1$ sits on the positive x-axis and positive angle runs counterclockwise. Radial guides fall at integer radii, i.e. at the perfect-square denominators $n = 1, 4, 9, 16, 25, 36$: each assigned annulus $A_n = \{\sqrt{n-1} < r \leq \sqrt{n}\}$ has area π, while shell n carries $\varphi(n)$ points. Prime shells have maximal residue occupancy ($\varphi(p) = p - 1$); denominators with many distinct small prime factors have lower normalized occupancy.

use it in every asset associated with this note: $\theta = 0$ points east along the positive x-axis, positive θ runs counterclockwise, $r = 0$ is the center, and $1/1$ sits on the positive x-axis.

The map is deliberately minimal — two elementary choices, radius $\sqrt{n}$ and angle $2\pi k/n$ — and the interest is entirely in what those two choices bring into view at once. We record four facts. Each is classical and is stated with its classical attribution; none is claimed as new. The layering is intentional: Section 2 recalls the exact structure the map displays, Section 3 places the display among known displays, and Section 4 states precisely what is and is not claimed.

2 What the map displays

2.1 Shell population is the totient

The number of admissible numerators on the shell of index n — the count of $k \in \{1,\dots,n\}$ with $\gcd(k,n) = 1$ — is by definition Euler's totient $\varphi(n)$ (OEIS A000010; the term *totient* is Sylvester's, 1879). Hence the shell of index n carries exactly $\varphi(n)$ points. It is useful to name the *residue occupancy*

$$\eta(n) = \frac{\varphi(n)}{n} = \prod_{p \mid n} \Big(1 - \frac{1}{p}\Big), \tag{2}$$

the fraction of residues modulo n that are admissible. Prime shells have maximal occupancy, $\varphi(p) = p - 1$ so $\eta(p) = 1 - 1/p$; denominators with many distinct small prime factors have lower occupancy (for instance $\eta(30) = \frac{8}{30}$, since $30 = 2 \cdot 3 \cdot 5$). Read outward, the fluctuation of $\varphi(n)$ — an erratic, toothed function of n, not a smooth ramp — is the fluctuation of shell population.

The totient shell is the organizing invariant of the author's Triangular-Fractional Grid series. In that setting the same φ counts arise as the entries of a *divisor band*, a geometric realization of the Gauss identity $\sum_{s \mid n} \varphi(s) = n$ [13]. The present rendering is a polar restatement of that shell structure; the proofs are given there and are not repeated here.

2.2 Angular positions are the primitive roots of unity

On the shell of index n, the angles $2\pi k/n$ taken over numerators k coprime to n are exactly the arguments of the primitive n-th roots of unity $e^{2\pi i k/n}$ — the $\varphi(n)$ roots of the n-th cyclotomic polynomial $\Phi_n(x)$ (classical; Gauss, *Disquisitiones Arithmeticae*, 1801). This identification — that $\gcd(k,n) = 1$ if and only if $e^{2\pi i k/n}$ is a primitive n-th root — is classical. The representational move made here is to use that identification as the angular layer of a denominator-stratified polar rendering, placing the primitive roots of order n on the distinct shell $r = \sqrt{n}$. The figure as a whole is then a concentric stack of primitive-root systems, one per denominator, in which the defining count of the cyclotomy — $\varphi(n)$ primitive roots among the n roots of $x^n - 1$, expressed by the factorization

$$x^n - 1 = \prod_{d \mid n} \Phi_d(x), \qquad \text{whence} \qquad n = \sum_{d \mid n} \varphi(d) \tag{3}$$

on comparing degrees — is read directly as the population of a shell. Equation (3) is the cyclotomic incarnation of the Gauss identity of Section 2.1.

One point of contact and contrast is worth stating. The standard cyclotomic picture places the n-th roots of unity on a single unit circle, dividing it into n equal arcs (the name *cyclotomic* is "circle-cutting"). The present rendering separates the primitive roots by denominator onto distinct concentric circles, so that the object seen is not a single divided circle but the family of primitive-root systems stratified by order. Figure 2 shows one such shell in full.

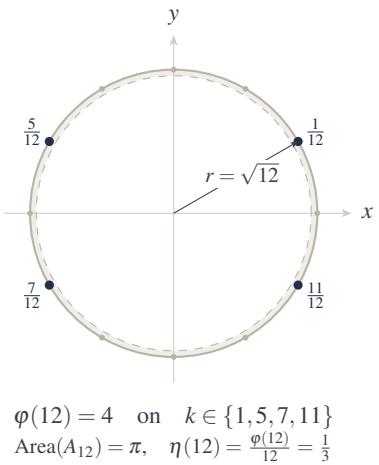

Figure 2: Anatomy of one shell, $n = 12$. The shell circle $r = \sqrt{12}$ (solid) and the inner boundary $r = \sqrt{11}$ (dashed) bound the assigned equal-area annulus A_{12} of area π. Of the 12 candidate directions $2\pi k/12$ (all shown), only the $\varphi(12) = 4$ coprime numerators $k \in \{1,5,7,11\}$ — the primitive 12th roots of unity — carry a point (navy). The residue occupancy is $\eta(12) = \varphi(12)/12 = 1/3$. One small figure exhibits denominator, totient, coprimality, primitive roots, the equal-area annulus, and occupancy at once.

2.3 Radial spacing makes equal-area shells

The disk of radius $\sqrt{n}$ has area πn. The annulus between successive shells,

$$A_n = \{\, z : \sqrt{n-1} < |z| \le \sqrt{n} \,\}, \qquad \text{Area}(A_n) = \pi\big(n - (n-1)\big) = \pi, \tag{4}$$

therefore has area π, independent of n: every denominator shell is assigned the same annular area. This is the equal-area radial law of Vogel's sunflower model [9], where seed n is placed at radius $c\sqrt{n}$ precisely so that each seed claims a constant area; the $\sqrt{n}$ law is what makes the sunflower's florets fill the head, and it is a Fermat spiral read in equal annular steps.

Two cautions are needed, because "equal area" is easily overread. First, Vogel's model places *one* seed per index n, whereas the present rendering places $\varphi(n)$ points on the shell of index n. The shared ingredient is the *radial* law $r = \sqrt{n}$, not a claim of uniform point density; we make this precise in Section 2.4. Second, the $\sqrt{n}$ law removes annulus-area distortion: differences in shell population are no longer confounded by unequal annular area. The radial law does not flatten arithmetic variation; it gives every denominator the same annular budget and lets $\varphi(n)$ supply the variation. This is the single design choice that binds the number-theoretic content of Sections 2.1–2.2 to the phyllotaxis tradition, and it is why we call the rendering *equal-area by denominator* rather than, more loosely, constant-density.

2.4 Cumulative population, densities, and the Farey length

The total number of points out to shell N is the summatory totient $\Phi(N) = \sum_{n=1}^{N} \varphi(n)$ (OEIS A002088). Two classical readings attach to it. First, $\Phi(N)$ counts the reduced fractions in $(0,1]$ with denominator at most N, so $1 + \Phi(N)$ is the length of the Farey sequence F_N of order N (the extra term counting $0/1$). Second, $\Phi(N)$ has the asymptotic

$$\Phi(N) = \frac{3}{\pi^2} N^2 + O(N \log N), \tag{5}$$

with leading constant $3/\pi^2 = 1/(2\zeta(2))$ (the Mertens asymptotic, 1874), the error term since sharpened to $O\big(N(\log N)^{2/3}(\log\log N)^{4/3}\big)$ (Walfisz's refinement, 1963); see also Hardy & Wright.

This asymptotic should not be misread as a constant-density filling of the disk. The subtlety is exactly the multiplicity of Section 2.3: shell n carries $\varphi(n)$ points, not one. Writing the plotted radius as $R = \sqrt{N}$, so that $N = R^2$, the cumulative count is

$$\Phi(N) = \Phi(R^2) \sim \frac{3}{\pi^2} R^4, \qquad \text{whence the average disk density} \qquad \frac{\Phi(R^2)}{\pi R^2} \sim \frac{3}{\pi^3} R^2 \tag{6}$$

grows with radius rather than staying constant. Because the plotted points lie on the circle $r = \sqrt{n}$ while the equal-area budget is an *annular* area, three per-shell notions of "density" must be kept apart; they answer different questions, and none of them is the number-theoretic visible-lattice density. We collect them.

Four densities, kept distinct

Shell population	$\#S_n = \varphi(n)$	
Annularly normalized shell density	$D_n^{\text{ann}} = \dfrac{\varphi(n)}{\pi}$	(population per assigned annular area)
Circumferential point density	$D_n^{\text{circ}} = \dfrac{\varphi(n)}{2\pi\sqrt{n}}$	(population per length of the circle $r = \sqrt{n}$)
Average disk density to radius R	$\dfrac{\Phi(R^2)}{\pi R^2} \sim \dfrac{3}{\pi^3} R^2$	

None of these is the number-theoretic visible-lattice density $1/\zeta(2) = 6/\pi^2$ *of* $\mathbb{Z}^2$.

Assigning shell n the equal-area annulus A_n of (4), its *annularly normalized population density* is $D_n^{\text{ann}} = \varphi(n)/\pi$. The rendered points themselves lie on the circle $r = \sqrt{n}$, however, whose circumferential density is $D_n^{\text{circ}} = \varphi(n)/(2\pi\sqrt{n})$. Thus the two notions should not be confused, because the rendered points themselves lie on the circle $r = \sqrt{n}$, not throughout the annulus; the two differ by the factor $\text{Area}(A_n)^{-1}$ versus $\text{circumference}^{-1}$, i.e. by $2\sqrt{n}$. In average order the shell population grows linearly with the denominator scale — since $\frac{1}{N}\sum_{n\le N}\varphi(n) \sim (3/\pi^2)N$ — while the annular area stays fixed; because φ is erratic, this is a statement about average order and not about any individual shell. The rendering therefore does not erase arithmetic density variation; it displays that variation without radial-area distortion. The parenthetical constant $3/\pi^2 = 1/(2\zeta(2))$ is half the density $6/\pi^2 = 1/\zeta(2)$ with which two integers are coprime, the factor one-half reflecting the restriction of the numerators to $k \le n$; that is a coprimality-density remark about $\mathbb{Z}^2$, distinct from the plotted areal density of (6).

2.5 Relation to the triangular-fractional grid

The rendering is the polar member of the author's Triangular-Fractional Grid (TFG) family, and the relationship is exact rather than merely one of family resemblance. For a TFG cell (N, K) write

$$g = \gcd(N, K), \qquad s = \frac{N}{g}, \qquad t = \frac{K}{g}, \tag{7}$$

so that $K/N = t/s$ in lowest terms. The reduced polar-skeleton projection is

$$\Pi_{\text{red}}(N, K) = \left(\sqrt{s},\ \frac{2\pi t}{s}\right), \tag{8}$$

and the composite $(N, K) \mapsto K/N = t/s \mapsto (\sqrt{s}, 2\pi t/s)$ sends every TFG cell to a point of the polar renderer. Multiple unreduced cells collapse onto the same reduced polar point: for example $(12, 8)$ gives $g = 4,\ s = 3,\ t = 2$, and $(6, 4)$ gives $g = 2,\ s = 3,\ t = 2$, so both land on $(\sqrt{3}, 4\pi/3)$. The polar renderer is thus the *reduced skeleton* of the TFG under denominator collapse (Figure 3) — a statement stronger and cleaner than "same grid, different radial law." In one sentence: the square grid supplies the cells, reduction supplies the denominator shell, the polar map supplies the coordinates, and the totient supplies the population.

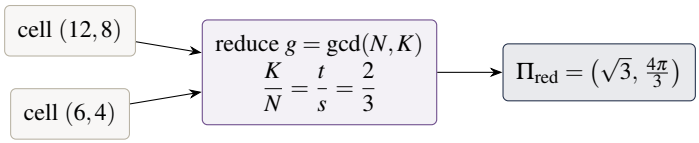

Figure 3: The TFG collapse to the polar skeleton. A cell (N,K) is reduced by $g = \gcd(N,K)$ to t/s, then mapped by $\Pi_{\text{red}}(N,K) = (\sqrt{s}, 2\pi t/s)$. The cells $(12,8)$ and $(6,4)$ both reduce to $2/3$ and therefore land on the same polar point $(\sqrt{3}, 4\pi/3)$. The renderer is the reduced skeleton of the grid.

3 Position among existing representations

The reduced fractions and the roots of unity are among the most-drawn objects in mathematics, and the rendering must be placed carefully against known pictures. The building blocks are classical without exception; the question is only whether the specific unified rendering — equal-area $\sqrt{n}$ shells populated by the primitive-root angles, with $\varphi(n)$ as the per-shell count and $\Phi(N)$ as the cumulative count — coincides with an existing one. The families below are the closest neighbours a targeted prior-art search returned; each is a cousin in one or two features, and the point of listing them is to record precisely which feature is shared and which is not.

Ford circles [2]. Encode the denominator of a reduced fraction p/q in a radius, placing at p/q a circle of radius $1/(2q^2)$ tangent to the real axis; the encoding is in the upper half-plane and by tangency, not in polar shells, and the per-denominator count is not made visible as a shell population.

Farey-sunburst constructions. Render Farey fractions as a Cartesian polygon whose vertex count is proportional to the summatory totient, and so share the cumulative-count content of Section 2.4, but are not a polar equal-area stratification by denominator.

Vogel's sunflower [9]. Supplies the $\sqrt{n}$ equal-area radius of Section 2.3, but its angular law is the golden angle and it carries no number-theoretic content; it is the phyllotaxis half of the present rendering without the arithmetic, and (as noted) places one seed per index rather than $\varphi(n)$.

Roots-of-unity diagrams. Place the n-th roots on a single unit circle and so carry the cyclotomic content of Section 2.2 for a fixed n, but are neither stratified by denominator nor equal-area, and do not display the totient as a count across orders.

The Ulam and Sacks prime spirals [7, 6]. Render the integers and highlight the primes on a spiral; the Sacks spiral in particular uses an Archimedean radius proportional to $\sqrt{n}$, so it shares the equal-area radial law, but it indexes single integers rather than reduced fractions and carries neither the primitive-root angles nor the totient shell-count.

Bacher's phyllotactic map [1]. The closest scholarly neighbour: the map $n \mapsto \sqrt{n}\, e^{2\pi i n\theta}$ with θ the golden ratio, which places $\sqrt{n}$-phyllotaxis in contact with the modular curve and a geodesic in $\mathrm{PSL}_2(\mathbb{Z})\backslash\mathbb{H}$. That map shares the $\sqrt{n}$ radius but runs a single integer index at a fixed irrational angle, rather than stratifying the reduced fractions by denominator with primitive-root angles; it is a different bridge between phyllotaxis and number theory, and the present rendering is offered as another.

Across these families, each known picture carries at most two of the three defining features of the rendering — equal-area $\sqrt{n}$ radius, primitive-root angle, totient shell-count — and none was found to carry all three at once. This is the sense, and the only sense, in which the rendering is offered as new; see Section 4.

4 Claims and non-claims

The rendering is the polar member of a family of coordinatizations that the author's Triangular-Fractional Grid series treats as costumes for one invariant, the totient shell. Its arithmetic backbone comprises the divisor-band bijection, the $\varphi(s)$ shell counts, the Gauss identity $\sum_{s|n} \varphi(s) = n$, and the floor-shell limit

$$\frac{1}{M^2} \sum_{m \le M} \varphi(m) \longrightarrow \frac{3}{\pi^2}.$$

These results are established in the arithmetic parent [13]. A square-spiral radial coordinatization of the same grid is given in [14]; the present rendering is a distinct radial map on the same underlying object, related to the cells by the exact collapse Π_{red} of Section 2.5, and is not that square spiral. A hexagonal (Eisenstein) sibling carries the same $\varphi(s)$ backbone under a hexagonal rendering [15]. The higher-dimensional lift, in which the shell count generalizes to the Jordan totient J_d with $\sum_{q|n} J_d(q) = n^d$ and the case $J_1 = \varphi$ recovers the present shells, is [16].

Separation from the earlier annular-shell diagnostic

The author's earlier paper *Annular Shell Isolation Near Zeta Zeros* [12] uses the word "shell" for a different mathematical object: zero-centered level sets

$$|\zeta(s)| = \frac{1}{m},$$

whose first-order local radius near a simple zero ρ is

$$r_m(\rho) \approx \frac{1}{m|\zeta'(\rho)|}.$$

Those analytic shells contract inward as m increases and are used to define a finite-range isolation diagnostic based on the local product $|\zeta'(\rho)|h_\rho$. The denominator shells of the present paper instead expand outward according to $r_n = \sqrt{n}$, carry exactly $\varphi(n)$ discrete points, and are assigned equal-area annuli of area π. The shared word "shell" therefore marks a common organizational grammar, not a shared shell law, invariant, or theorem. Figure 4 records the distinction visually.

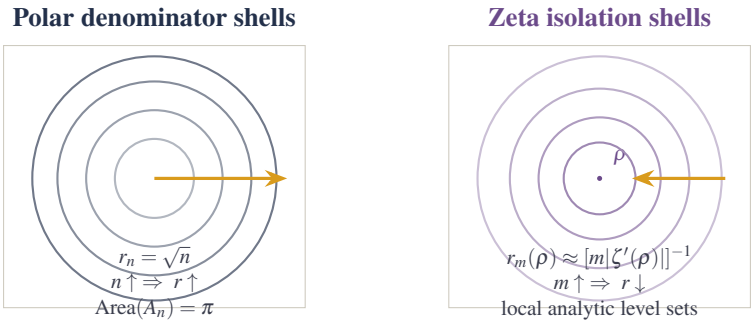

Figure 4: Two distinct uses of shell coordinates in the author's corpus. The present polar renderer assigns reduced fractions to outward-growing denominator shells $r_n = \sqrt{n}$ with constant assigned annular area π. The earlier zeta diagnostic uses inward-contracting local level shells with first-order radius $r_m(\rho) \approx 1/(m|\zeta'(\rho)|)$ around a known simple zero. The comparison is organizational only: no common shell law or invariant is asserted.

It remains to state the claim precisely, in the layered discipline of the series. Nothing in Sections 2 or 4 is asserted as a new theorem: the totient shell-count, the primitive-root angular positions, the equal-area $\sqrt{n}$ spacing, and the summatory-totient asymptotic are classical, with the attributions given above, and the divisor-band content is proved in the cited corpus record.

Representational contribution. *The placement of the reduced fractions at* $(\sqrt{n}, 2\pi k/n)$ *so that the four classical structures of Section 2 are read together in one equal-area figure; and, within that, the equal-area-by-denominator choice as the design decision that binds the number-theoretic reading to the phyllotaxis reading, together with the exact denominator-collapse map* Π_{red} *that realizes the rendering as the reduced skeleton of the triangular-fractional grid.*

On the status of that contribution we are deliberately cautious: a targeted survey found no prior instance of the specific unified rendering, but the building blocks are elementary and heavily drawn, and the absence of a found instance is not a proof of novelty; an unindexed figure, applet, or note may predate it. Accordingly the rendering is presented as an authored lens on classical structure, offered for its clarity in bringing the totient, the cyclotomy, the equal-area law, and the Farey count into a single view, and not as a claim upon any of the mathematics it renders. It is a lens, not a law.

An interactive version of the rendering is available at `https://cerebralgraphix.com/tools/polar_shell_renderer`.

References

[1] R. Bacher, "On geodesics of phyllotaxis," *Confluentes Mathematici* **6** (2014), no. 1, 3–27. arXiv:1301.7568.

[2] L. R. Ford, "Fractions," *American Mathematical Monthly* **45** (1938), no. 9, 586–601.

[3] C. F. Gauss, *Disquisitiones Arithmeticae*, 1801 (Sec. VII, on the cyclotomy).

[4] G. H. Hardy and E. M. Wright, *An Introduction to the Theory of Numbers*, 5th ed., Oxford University Press, 1979.

[5] F. Mertens, "Ueber einige asymptotische Gesetze der Zahlentheorie," *Journal für die reine und angewandte Mathematik* **77** (1874), 289–338.

[6] R. Sacks, "Number spiral" (2003), self-published, `numberspiral.com`.

[7] M. L. Stein, S. M. Ulam, and M. B. Wells, "A visual display of some properties of the distribution of primes," *American Mathematical Monthly* **71** (1964), no. 5, 516–520.

[8] J. J. Sylvester, "On certain ternary cubic-form equations," *American Journal of Mathematics* **2** (1879), 357–393 (the word *totient*, p. 361).

[9] H. Vogel, "A better way to construct the sunflower head," *Mathematical Biosciences* **44** (1979), no. 3–4, 179–189.

[10] A. Walfisz, *Weylsche Exponentialsummen in der neueren Zahlentheorie*, VEB Deutscher Verlag der Wissenschaften, Berlin, 1963.

[11] OEIS Foundation, sequences A000010 (Euler totient φ) and A002088 (summatory totient Φ).

[12] J. Huckstead, *Annular Shell Isolation Near Zeta Zeros*, Zenodo, June 5, 2026, DOI 10.5281/zenodo.20564213.

[13] J. Huckstead, *Divisor-Band Bijections and Totient Shells in the Triangular-Fractional Grid*, Zenodo, DOI 10.5281/zenodo.21187177.

[14] J. Huckstead, *A Radial Coordinatization of the Triangular-Fractional Grid*, Zenodo, DOI 10.5281/zenodo.21186245 (square-spiral radial sibling — distinct radial map).

[15] J. Huckstead, *The Hexagonal Coil: An Eisenstein Sibling of the Triangular-Fractional Grid*, Zenodo, DOI 10.5281/zenodo.21210741 (hexagonal sibling; same $\varphi(s)$ backbone).

[16] J. Huckstead, *The Jordan Chamber Lift: Higher-Dimensional Denominator Shells via the GCD Collapse*, Zenodo, DOI 10.5281/zenodo.20580136 (higher-dimensional lift; $J_1 = \varphi$).